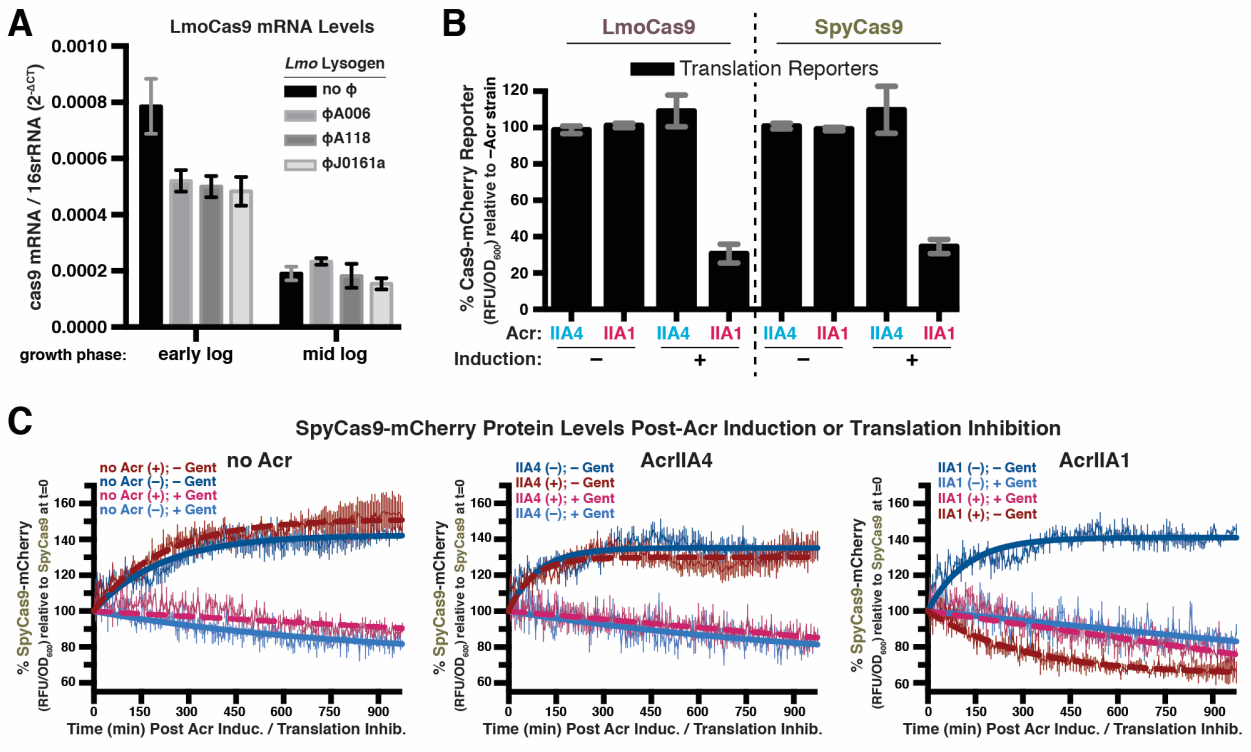

Figure S1. AcrIIA1 Stimulates Post-transcriptional Degradation of Lmo and Spy Cas9 in *Listeria*, Related to Figure 1

(A) Cas9 mRNA levels of *Lmo*10403s lysogens containing the indicated prophages in early or mid-log phase as quantified by qRT-PCR. Transcript measurements were conducted in technical triplicate and data are shown as the mean $2^{-\Delta CT}$ values normalized to the 16S rRNA endogenous control gene ± SD (error bars). (B) Lmo or Spy Cas9-mCherry protein levels in *Lmo*10403s expressing Lmo or Spy Cas9-mCherry from the constitutively active pHyper promoter and AcrIIA1 or AcrIIA4 from an inducible promoter. Cas9-mCherry measurements reflect the mean percentage mCherry (RFU/OD_{600}) in cells treated with 100 mM rhamnose (+, induced Acr) or glycerol (–, uninduced Acr), relative to a control strain lacking an Acr (–Acr). Error bars represent the mean ± SD of three biological replicates. (C) SpyCas9-mCherry protein levels post Acr induction or translation inhibition. *Lmo*10403s expressing SpyCas9-mCherry from the constitutively active pHyper promoter and AcrIIA1 or AcrIIA4 from an inducible promoter were grown to mid-log and treated with 100 mM rhamnose to induce Acr expression (+, dashed lines) or 100 mM glycerol as a neutral carbon source control (–, solid lines) and 5 µg/mL gentamicin (Gent) to inhibit translation (+) or water (–) as a control. SpyCas9-mCherry protein measurements reflect the mean percentage fluorescence (RFU/OD_{600}) relative to the SpyCas9-mCherry levels at the time translation inhibition was initiated (0 min). Error bars (vertical lines) represent the mean ± SD of at least three biological replicates. Data were fitted by nonlinear regression to generate best-fit decay curves. Note: *Lmo* doubling time is significantly slower in LB media containing glycerol and/or rhamnose carbon sources (Fieseler et al., 2012).

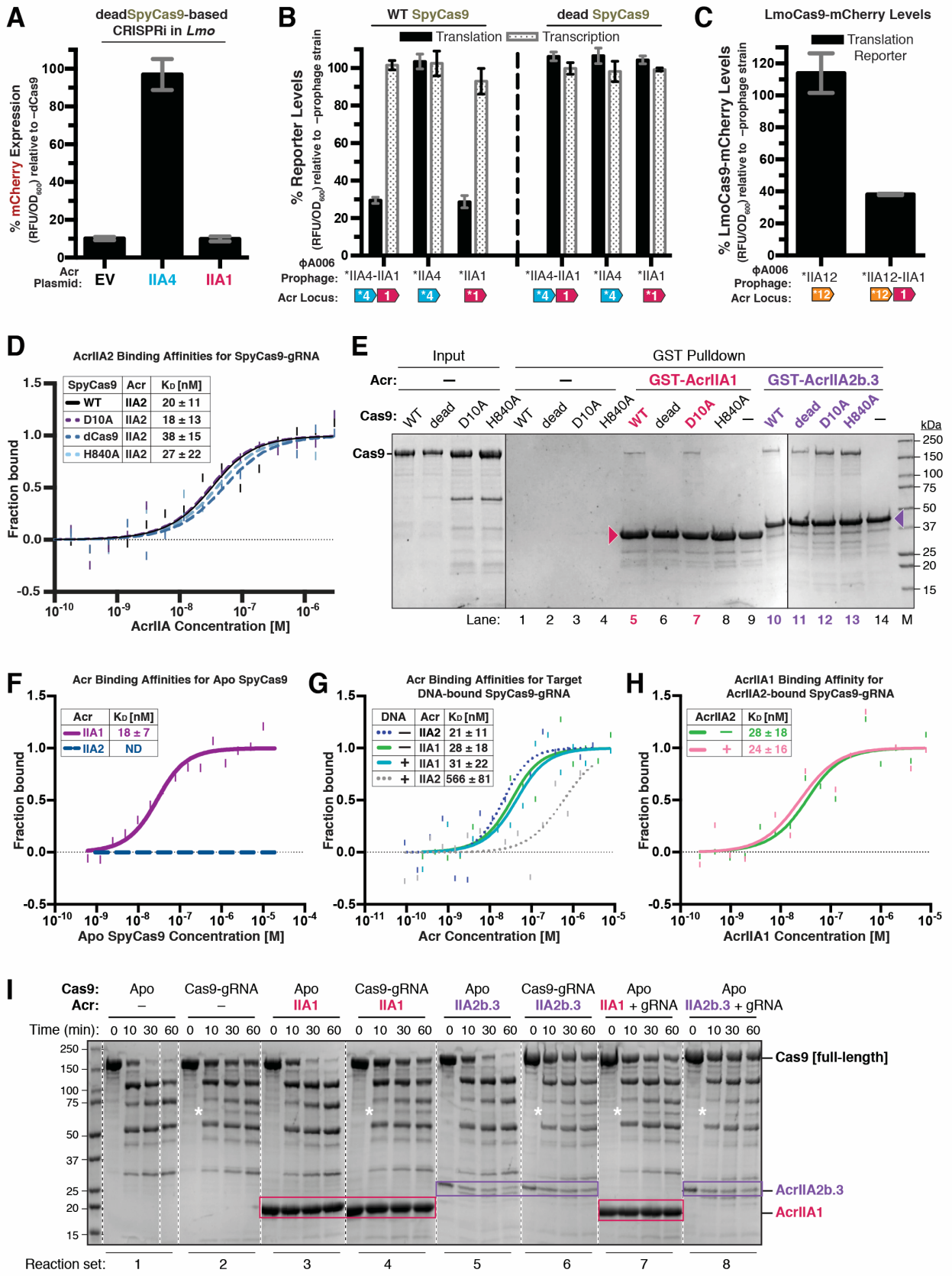

Figure S2. AcrIIA1 Selectively Binds and Inactivates Catalytically Active Cas9, Related to

Figure 2
(A) Acr-mediated inhibition of CRISPRi in *Lmo*10403s containing a chromosomally-integrated construct expressing deadSpyCas9 from the inducible pRha-promoter and sgRNA that targets the pHelp-promoter driving mCherry expression. mCherry expression measurements reflect the mean percentage fluorescence (RFU/OD_{600}) in deadCas9-induced cells relative to uninduced (–dCas9) controls of three biological replicates ± SD (error bars). (B) Translational and transcriptional reporter levels of catalytically active and dead SpyCas9 in *Lmo*10403s lysogenized with isogenic ΦA006 prophages encoding the indicated Acrs. (C) Catalytically active LmoCas9-mCherry protein levels in *Lmo*10403s lysogenized with isogenic ΦA006 prophages encoding AcrIIA12 alone or with AcrIIA1. Cas9-mCherry (translational reporter, black bars in B and C) or mCherry (transcriptional reporter, gray bars in B) measurements reflect the mean percentage mCherry ($RFUs/OD_{600}$) in the indicated lysogens relative to the control strain lacking a prophage (–prophage). Error bars represent the mean ± SD of at least three biological replicates (B and C). Asterisk (*) indicates the native orfA RBS (strong) in ΦA006 was used for Acr expression. (D) Quantification of the binding affinities (K_D; boxed inset) of AcrIIA2b.3 for WT, catalytically dead (dCas9), or nickase (D10A or H840A) SpyCas9-gRNA complexes using microscale thermophoresis. Data shown are representative of three independent experiments. Note: Data for WT Cas9-gRNA is duplicated from Figure 2D for easy comparison. (E) Differential interactions of SpyCas9 nickases with AcrIIA1. GST-tagged AcrIIA1 (magenta arrowhead, lanes 5-9) or AcrIIA2b.3 (purple arrowhead, lanes 10-14) were incubated with SpyCas9-gRNA complexes (WT, dead, D10A, H840A; input) and pulled down with glutathione-coupled beads. WT and D10A Cas9-gRNA co-purify with AcrIIA1 (lanes 5 and 7), whereas dead and H840A Cas9-gRNA do not (lanes 6 and 8). All four Cas9-gRNA complexes co-purify with AcrIIA2b.3 (lanes 10-13). Cas9-gRNA complexes were incubated with beads in the absence of GST-Acr proteins to test for non-specific binding (lanes 1-4). M, molecular weight marker. (F-H) Quantification of the binding affinities (K_D; boxed insets) of AcrIIA1 and AcrIIA2b.3 for Apo or gRNA-bound SpyCas9 (F), SpyCas9-gRNA pre-bound to target DNA (G), and SpyCas9-gRNA pre-bound to AcrIIA2b.3 (H) using microscale thermophoresis. ND indicates no binding was detected. Data shown are representative of three independent experiments. Note: The same data for the Cas9-gRNA-AcrIIA1 binding control (K_D = 28 ± 18 nM) is displayed in both G and H for easy comparison. (I) Limited α-chymotrypsin proteolysis of SpyCas9-Acr complexes. Proteolysis of Apo SpyCas9 (set 1) or SpyCas9-gRNA (set 2) without anti-CRISPR (–) or in the presence of AcrIIA1 (sets 3, 4, 7; magenta boxes) or AcrIIA2b.3 (sets 5, 6, 8; purple boxes). For reaction sets 7 and 8, Apo Cas9 was first incubated with anti-CRISPR followed by addition of gRNA. (*) Denotes a proteolysis product that appears in all Cas9-gRNA reactions but not Apo Cas9 reactions. Dashed lines indicate where intervening lanes were removed for clarity.

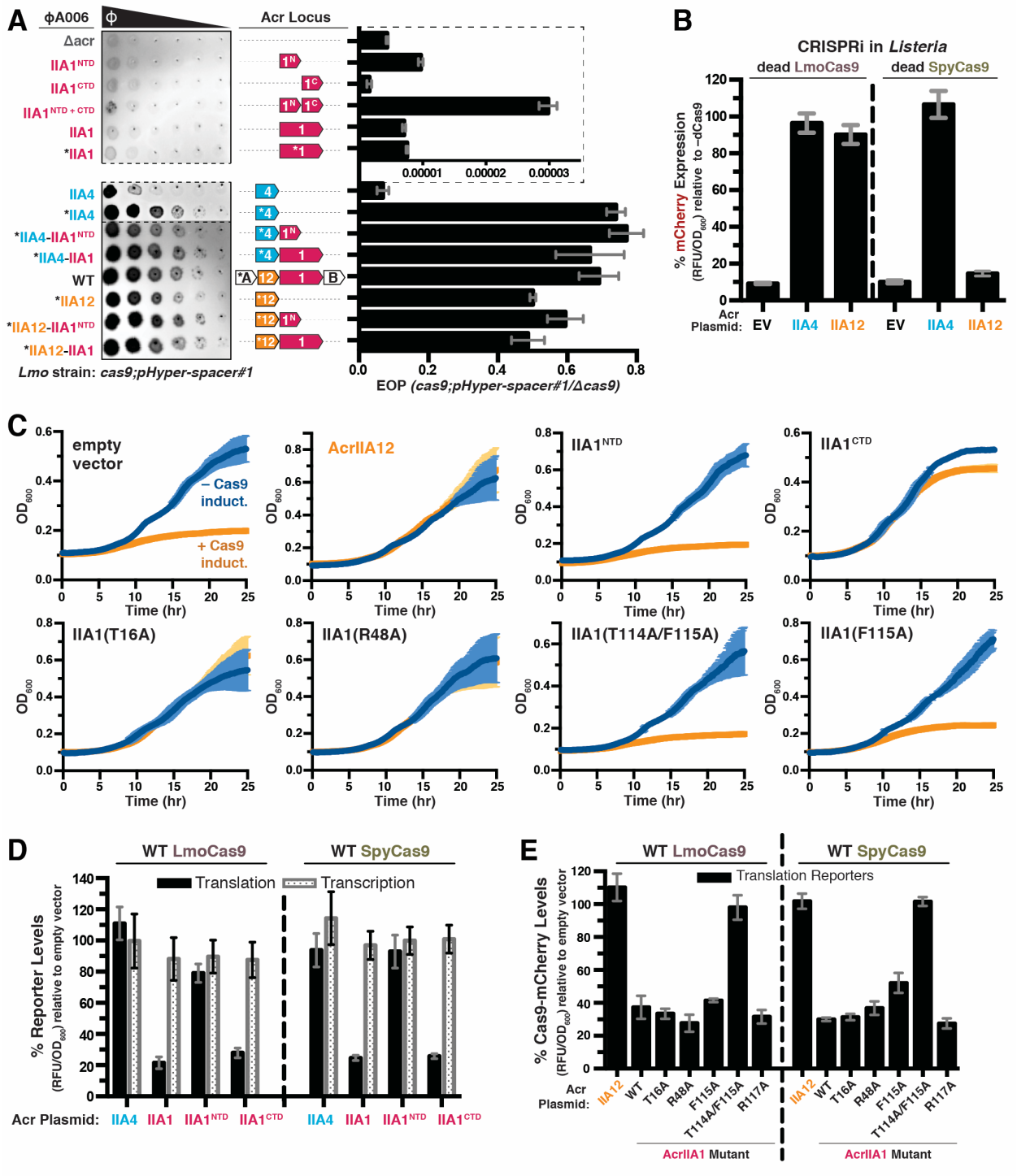

Figure S3. AcrIIA1^{CTD} Inactivates Cas9 in Self-Targeting *Listeria* Strains and a Coexisting Acr Blocks Cas9 During Phage Lytic Replication, Related to Figures 3 and 4

(A) Left: Representative image of plaquing assays where isogenic ΦA006 phages are titrated in ten-fold serial dilutions (black spots) on a lawn of *Lmo*10403s (gray background). Dashed lines indicate where intervening rows were removed for clarity. Right: Efficiency of plaquing (EOP) of isogenic ΦA006 phages expressing the indicated Acrs on *Lmo*10403s. Plaque forming units (PFUs) were quantified on *Lmo*10403s overexpressing the first spacer in the native CRISPR

array that targets ΦA006 (*cas9;pHyper-spacer#1*) and normalized to the number of PFUs measured on a non-targeting *Lmo*10403s-derived strain (*Δcas9*). The dashed lines boxing the first 6 phages show a zoomed in view of the graph with a distinct x-axis scale. Data are displayed as the mean EOP of at least three biological replicates ± SD (error bars). Note: this figure contains the same subset of data displayed in Figure 3A. (B) Anti-Cas9 activity of AcrIIA12 in a *Lmo*10403s CRISPRi strain expressing Lmo or Spy deadCas9 from the inducible pRha-promoter and sgRNA that targets the pHelp-promoter driving mCherry expression. Measurements reflect the mean percentage mCherry expression (RFU/OD_{600}) in deadCas9-induced cells relative to uninduced (–dCas9) controls of three biological replicates ± SD (error bars). Note: AcrIIA12 inhibits Lmo but not Spy deadCas9-based CRISPRi, indicating specificity against LmoCas9. (C) Anti-Cas9 activity in *Lmo*10403s self-targeting strains containing Acr-expressing plasmids and chromosomally-integrated constructs expressing LmoCas9 from the inducible pRha-promoter and sgRNA that targets the bacterial chromosome. Bacterial growth was monitored after LmoCas9 induction (orange lines) or no induction (blue lines) and data are displayed as the mean OD_{600} of three biological replicates ± SD (error bars). (D-E) Translational (black bars in D and E) and transcriptional (gray bars in D) reporter levels of catalytically active Lmo and Spy Cas9 in *Lmo*10403s containing plasmids expressing Acrs. Cas9-mCherry (translational reporter) and mCherry (transcriptional reporter) measurements reflect the mean percentage mCherry (RFU/OD_{600}) in the presence of the indicated Acrs relative to the control strain containing an empty vector of three biological replicates ± SD (error bars).

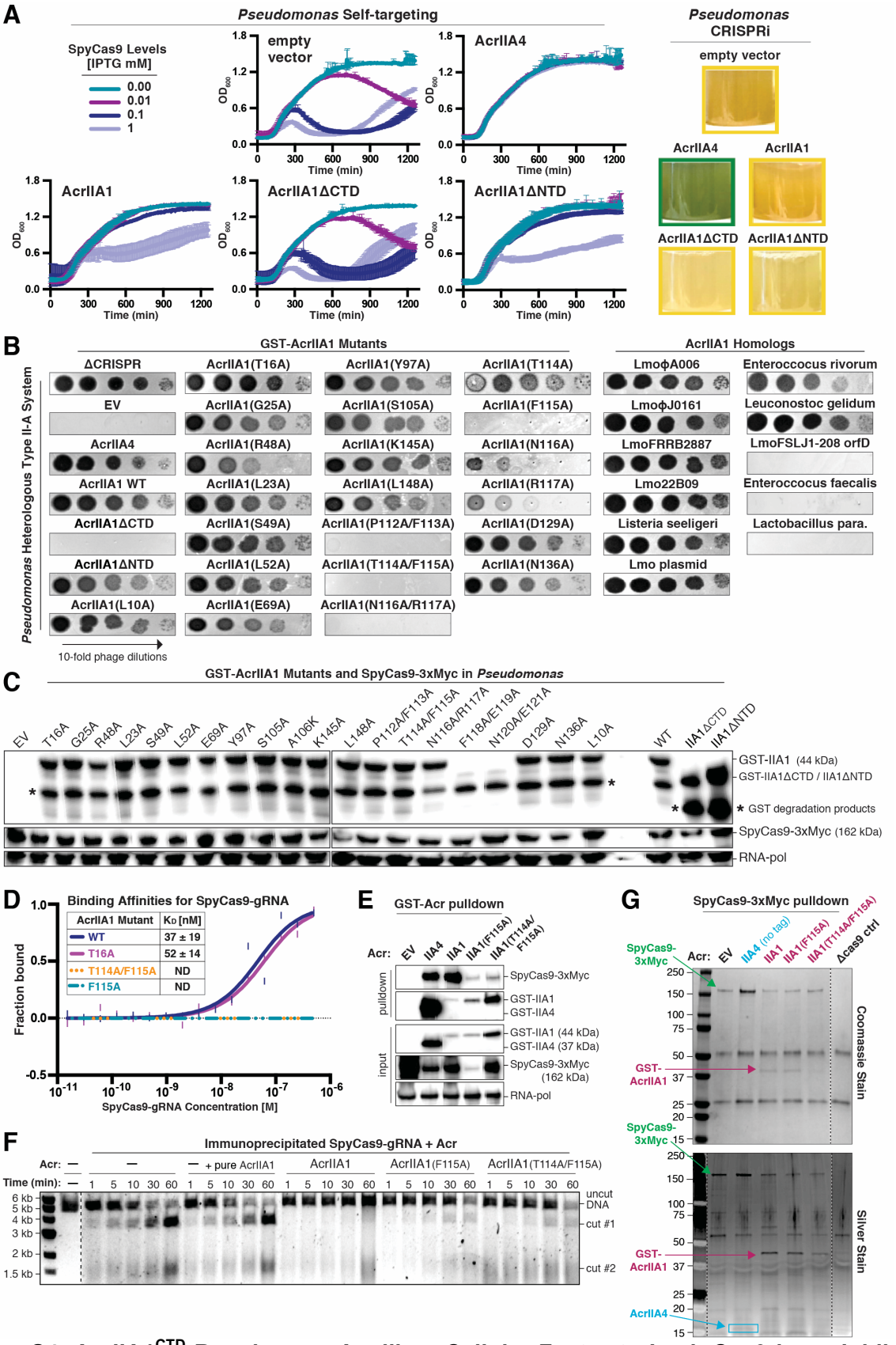

Figure S4. AcrIIA1^{CTD} Requires an Auxiliary Cellular Factor to Lock Cas9 in an Inhibited

State, Related to Figure 4

(A) Anti-Cas9 activity in *P. aeruginosa* self-targeting (left) and CRISPRi (right) strains containing plasmids expressing Acrs and chromosomally-integrated SpyCas9-sgRNA programmed to target the *phZM* gene promoter. For self targeting (left), SpyCas9 expression from the inducible pLAC-promoter was titrated using the indicated IPTG concentrations and bacterial growth curves display the mean OD_{600} of three biological replicates ± SD (error bars). CRISPRi (right) was qualitatively assessed by inspecting culture pigment. Transcriptional repression of the *phzM* gene by dCas9 generates a yellow culture whereas inhibition of dCas9 (e.g. by an Acr) allows *phzM* expression and pyocyanin production that generates a green culture. Representative pictures of three biological replicates are shown. (B) Plaquing assays where the *P. aeruginosa* DMS3m-like phage JBD30 is titrated in ten-fold dilutions (black spots) on a lawn of *P. aeruginosa* (gray background) expressing the indicated Acrs and Type II-A SpyCas9-sgRNA programmed to target phage DNA. Representative pictures of 3 biological replicates are shown. (C) Immunoblots detecting GST-tagged AcrIIA1 (mutants or individual domains) proteins, Myc-tagged SpyCas9 protein, and RNA-polymerase as a protein loading control in a *P. aeruginosa* strain heterologously expressing the Type II-A SpyCas9-gRNA system and the indicated Acrs. (*) Denotes GST-containing degradation products derived from GST-tagged Acr proteins. AcrIIA1 mutants that failed to express were not analyzed further. (D) Quantification of the binding affinities (K_D; boxed inset) of WT and mutant AcrIIA1 proteins with SpyCas9-gRNA using microscale thermophoresis. ND indicates no binding detected. Data shown are representative of three independent experiments. (E) Immunoblots detecting 3xMyc-tagged SpyCas9 protein that co-immunoprecipitated with GST-tagged Acrs in a *P. aeruginosa* strain heterologously expressing Type II-A SpyCas9-gRNA and the indicated Acrs. For input samples, one-hundredth lysate volume was analyzed to verify tagged protein expression and RNA-polymerase was used as a loading control. Representative blots of three biological replicates are shown. (F) Time course of SpyCas9 DNA cleavage reactions conducted with SpyCas9-gRNA-Acr complexes immunoprecipitated from *P. aeruginosa*. A reaction with SpyCas9-gRNA immunoprecipitated without an Acr (–) was supplemented with recombinant WT AcrIIA1 protein purified from *E. coli* (+ pure AcrIIA1). Dashed line indicates where intervening lanes were removed for clarity. Data shown are representative of three independent experiments. (G) SDS-PAGE and Coomassie Blue staining analysis of SpyCas9-gRNA-Acr complexes immunoprecipitated from *P. aeruginosa*.

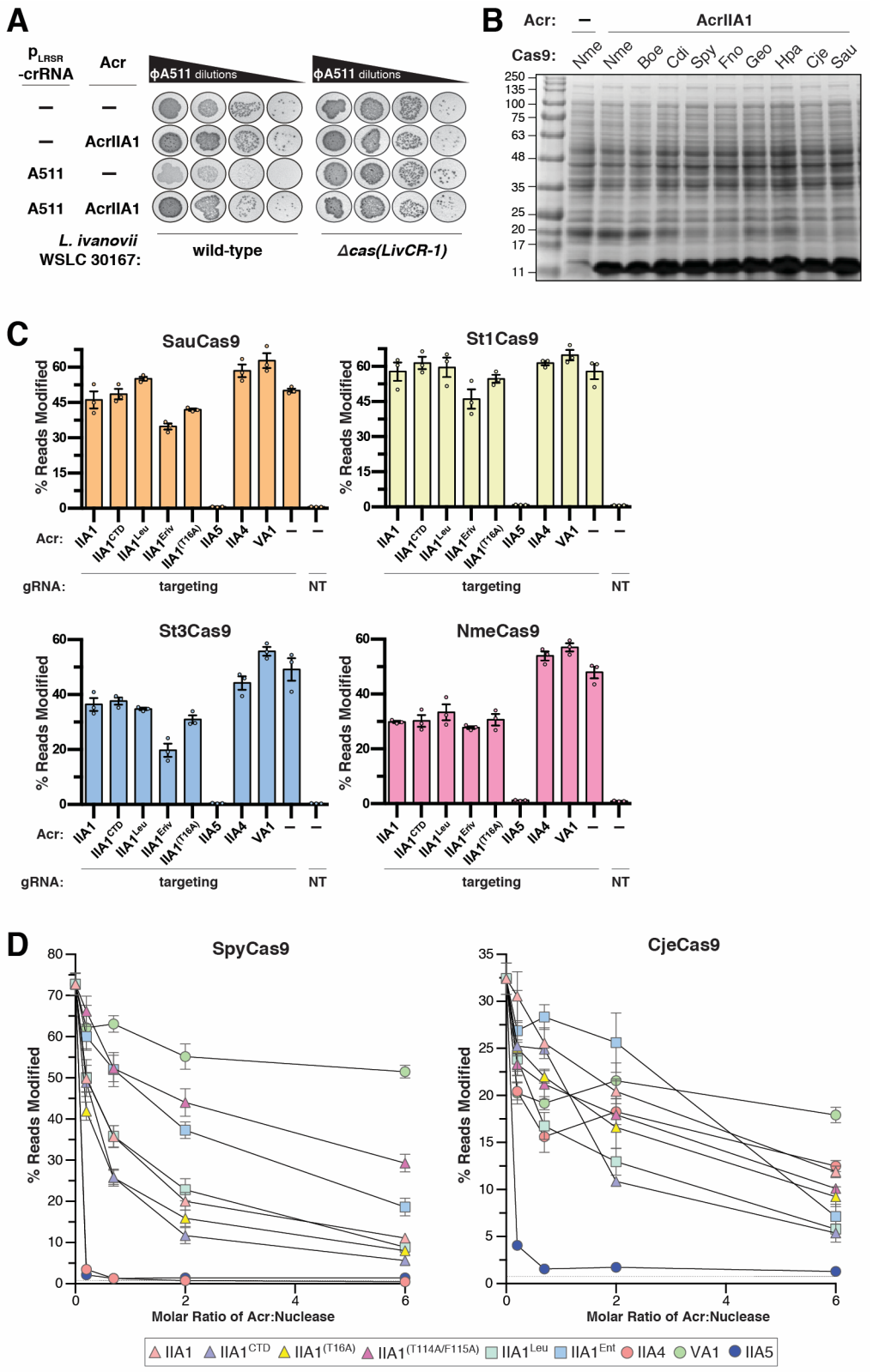

Figure S5. AcrIIA1 Inhibition of Cas9 Orthologues in Heterologous Hosts, Related to Figure 5

(A) Plaquing assays where the *Listeria* phage ΦA511 is titrated in ten-fold serial dilutions (black spots) on lawns of the *Listeria ivanovii* WSLC 30167 (gray background) strain with an endogenous Type II-A LivCas9 system or lacking this system (*Δcas*), plasmid-expressed AcrIIA1 or no Acr (–), and crRNA that targets phage DNA or a non-targeting control (–) expressed from the pLRSR plasmid. (B) SDS-PAGE and Coomassie Blue staining analysis of AcrIIA1 expression after IPTG induction in *E. coli* strains containing the indicated Cas9 orthologues. (C) Gene editing activities of Cas9 orthologues in human cells in the presence of AcrIIA1 variants and orthologues. Control inhibitors (references in Methods): AcrIIA4 selective inhibitor of SpyCas9; AcrIIA5 broad-spectrum Cas9 inhibitor; AcrVA1 Cas12 inhibitor (negative control for Cas9 orthologues). Editing assessed by targeted sequencing; NT indicates a no-sgRNA control condition; error bars indicate SEM for three independent biological replicates. (D) Activities of SpyCas9 and CjeCas9 in human cells in the presence of varying doses of acr plasmid (molar ratios of 6:1, 2:1, 0.67:1, and 0.22:1 acr:nuclease). Gene editing assessed by targeted sequencing. Error bars indicate SEM for three independent biological replicates.

Table S1. AcrIIA1 homolog protein accession numbers, Related to Figure 4

Strains Containing AcrIIA1 Homologs	Designated Homolog Name	Protein Accession #
Listeria monocytogenes J0161	Lmoϕ A006/ϕJ0161	WP_003722518.1
Listeria monocytogenes strain LMO10	LMO10	KUG37233.1
Listeria monocytogenes strain FRRB 2887	LmoFRRB2887	WP_085696370.1
Listeria monocytogenes isolate 22B09	Lmo22B09	WP_077316628.1
Listeria seeligeri FSL S4-171	Listeria seeligeri	EFS02359.1
Enterococcus rivorum strain LMG 258993	E. rivorum	WP_069698591.1
Listeria monocytogenes CFSAN026587 plasmid	Lmo plasmid	WP_061665673.1
Leuconostoc gelidum subsp. gasicomitatum KG16-1	Leu gelidum	CUR63869.1
Lactobacillus parabuchneri strain FAM23166	Lac parabuchneri	WP_084975236.1
Enterococcus faecalis strain plasmid Efsorialis-p2	E. faecalis	WP_002401838.1
Listeria monocytogenes SLCC2540, serotype 3b	Lmo orfD	WP_012951927.1